Applied Catalysis B: Environmental 158–159 (2014) 70–75

Contents lists available at ScienceDirect

Applied Catalysis B: Environmental

journal homepage: www.elsevier.com/locate/apcatb

Scandium substituted nickel–cobalt ferrite nanoparticles for catalyst applications

Nicolae Rezlescu[a,*], Elena Rezlescu[a], Paul Dorin Popa[a], Corneliu Doroftei[a], Maria Ignat[b]

[a] National Institute of Research and Development for Technical Physics, Iasi, Romania
[b] "Al. I. Cuza" University, Faculty of Chemistry, Iasi, Romania

ARTICLE INFO

Article history:
Received 15 January 2014
Received in revised form 24 March 2014
Accepted 29 March 2014
Available online 5 April 2014

Keywords:
Ferrite
Sc-substitution
Catalyst
Self-combustion
Nanostructure

ABSTRACT

Nanograined $Ni_{0.5}Co_{0.5}Sc_xFe_{2-x}O_4$ ($x = 0$, 0.05, 0.1 and 0.2) spinel ferrites were prepared by sol–gel self-combustion method and heat treatment at 900 °C for 4 h. Their structure and surface properties were investigated by X-ray diffraction, scanning electron microscopy, EDX spectroscopy and BET analysis. The catalyst properties of the ferrite nanopowders were tested in the catalytic combustion of acetone, propane and benzene. The results revealed that the partial substitution of Fe^{3+} by Sc^{3+} ions on the octahedral sites of spinel structure of $Ni_{0.5}Co_{0.5}Fe_2O_4$ ferrite has a favorable effect on the catalytic activity of this ferrite. The $Ni_{0.5}Co_{0.5}Sc_{0.2}Fe_{1.8}O_4$ ferrite composition was found to be the most active catalyst and can be a good candidate for catalytic combustion of propane and acetone at moderate temperatures. The acetone conversion over this catalyst exceeds 90% at 400 °C. The enhancement of the catalytic activity of the Sc doped Ni–Co ferrites may be ascribed to smaller crystallite sizes (35–39 nm), larger specific surface areas (29–32 m^2/g) and the presence of Sc cations in spinel structure.

1. Introduction

The progressive increase of volatile organic compound (VOC) emissions induces the development of new methods for their abatement from air [1–3]. In comparison with conventional thermal oxidation, catalytic combustion is considered one of the most promising technologies for VOC removal [2,4]. Catalytic combustion is a more economical process that can operate at low temperature (<500 °C) with dilute effluent streams (<1% VOC) [4]. The performance of catalytic combustion strongly depends on the catalyst used. Two categories of catalysts are generally employed for VOC catalytic oxidation reaction: (i) noble metal (Pt, Pd, Rh) and (ii) transition metal oxides.

In the recent years many efforts have been directed toward producing catalytic materials based on simple and mixed transition-metal oxides to replace the expensive noble metal catalysts. Metal oxide catalysts, although less active than noble metal catalysts, have certain advantages, such as low price, earthly abundance, high chemical and thermal stability, high resistance to poisoning and the easy way of preparation [5–11]. Spinels and perovskites are the most studied oxide compounds in the context of VOC catalytic combustion. As a novel catalytic material, oxide compounds, called spinel ferrites, are extensively investigated as catalysts in the flameless combustion of volatile organic compounds (VOCs) [12–15].

Ferrites are mixed transition metal oxide compounds with a spinel cubic structure and can be described by the general formula $M^{2+}Fe_2{}^{3+}O_4$, where M^{2+} is a divalent metal ion. The spinel configuration is based on a face centered cubic lattice of oxygen ions, forming tetrahedral (A) and octahedral (B) sites that may be occupied either by M^{2+} and/or Fe^{3+} ions. In normal ferrite, M^{2+} ions occupy the tetrahedral sites and Fe^{3+}occupy the octahedral sites. If divalent cations M^{2+} occupy the octahedral sites and Fe^{3+} cations are distributed among tetra and octahedral sites, the spinel is called inverse spinel [16].

The catalytic properties of the spinel ferrites are influenced by the distribution of cations among the octahedral and tetrahedral sites in the spinel structure [15]. Jacobs et al., [17] suggested that in the spinel structure, the octahedral sites are almost exclusively exposed at the surface of the spinel crystallite and that the catalytic activity is mainly due to octahedral cations.

The preparation of spinel ferrites as nanopaticles is of high interest because they exhibit improved physico-chemical properties for catalytic combustion applications. The smaller the particle size, the larger the surface area is in front of gases. There is a variety of methods [10,18–25] for preparing the nanocrystalline ferrites. For any practical wide-scale application, the price of catalyst has

* Corresponding author. Tel.: +40 0232216895; fax: +40 0232231132.
E-mail addresses: nicolae.rezlescu@gmail.com, reznic@phys-iasi.ro (N. Rezlescu).

http://dx.doi.org/10.1016/j.apcatb.2014.03.052
0926-3373/

to be reasonably low. To meet this demand, simple and inexpensive methods of ferrite synthesis appear to be attractive. In the present study a non-conventional procedure, sol–gel coupled with self-combustion, was used [10]. This combined method implies a low cost and allows the preparation of the ferrite nanoparticles with molecular scale homogeneity over a wide range of particle size.

The objectives of this work were to synthesize nanosize-structured scandium containing Ni–Co ferrites and also to evaluate their catalytic activity in the VOC combustion. Until now the catalyst properties of Sc doped Ni–Co ferrites prepared by sol–gel self-combustion have not been investigated. Lei Ze et al. [26] have investigated catalytic activity of Sc-doped $La_{0.8}Sr_{0.2}Fe_{1-x}Sc_xO_{3-d}$ perovskite ($x = 0–1$) for methane combustion and good catalytic activity was obtained at a Sc doping of 0.5. Hosseini et al. [27] investigated the catalytic activity of Ni–Co ferrite on the growth of carbon nanotube and indicated an inverse spinel structure for Ni–Co ferrite. This means that Ni^{2+} and Co^{2+} cations occupy the octahedral sites and Fe^{3+} cations occupy octahedral and terahedral sites equally. This cation distribution favors the availability of catalytic sites exposed at the surface of the spinel crystallites [17]. Pakhomova et al. [28] evidenced by magnetic measurements that Sc^{3+} ions prefer the octahedral sites only.

The structural and catalytic properties of Sc containing Ni–Co ferrites, $Ni_{0.5}Co_{0.5}Sc_xFe_{2-x}O_4$ ($x = 0$, 0.05, 0.1 and 0.2), were investigated by X-ray diffraction (XRD), scanning electron microscopy (SEM), BET surface area measurements, energy-dispersive X-ray spectroscopy (EDX) and catalytic flameless combustion of acetone, benzene and propane.

Our study can have applications in finding a suitable candidate of doped ferrite nanocrystals as catalyst for combustion of VOCs.

2. Experimental

2.1. Preparation of the catalyst materials

In this paper $Ni_{0.5}Co_{0.5}Sc_xFe_{2-x}O_4$ ($x = 0$, 0.05, 0.1 and 0.2) ferrite nanocrystals were prepared by sol–gel self-combustion route [29] which offers a homogeneous mixing (considering the very small scandium additions) and the control of the grain size by subsequent heat treatment. It is not possible to replace much of the Fe by Sc ions because the ionic radius of Sc^{3+} (0.088 nm) is much greater than the radius of Fe^{3+} (0.069 nm) [30].

Metal nitrates were used as precursors. The preparing method included the following steps: (1) dissolution of metal nitrates in deionized water; (2) polyvinyl alcohol (10% concentration) addition to nitrate solution to make a colloidal solution; (3) NH_4OH (10% concentration) addition to increase pH to about 8; a sol of metal hydroxides in polyvinyl alcohol and ammonium nitrate were obtained; (4) stirring at 80 °C for 10 min to turn the sol of metal hydroxides into viscous gel; (5) drying the gel at 100 °C for 12 h; (6) self-combustion; the dried gel was locally ignited by an electrically heated wire and an exothermic reaction takes place. Once initiated, the combustion wave spontaneously auto propagated (less than 30 s) through the dried gel and results a loose powder. During the combustion reaction the temperature is of about 1000 °C and the nucleation of very fine crystallites takes place; (7) calcination at 550 °C for 15 min of the burnt powder to eliminate any residual organic compound; (8) heat treatment of the calcined powders at 900 °C for 4 h, in air, to achieve a complete crystallization of ferrites.

2.2. Catalysts characterization

The crystal structure and phase composition of the samples were analyzed by XRD. X-ray diffraction measurements of the powders were performed at room temperature using PANALYTICAL X' PERT PRO MPD powder diffractometer and CuKα radiation. The spectra were scanned between 20 and 80° (2θ) at a rate of 2 °/min. The average crystallite size was evaluated based on XRD peak broadening using the Scherer equation $D = 0.9\lambda/\beta\cos\theta$, were λ is radiation wavelength (0.15405 nm) of CuKα, β is the half width of the peak and θ is the Bragg diffraction peak angle. A scanning electron microscope (JEOL-200 CX) was used to visualize the surface morphology. A Quantachrome automated gas adsorption system (Quantachrome Instruments) was used to obtain N_2 adsorption isotherms at 77 K. The BET specific surface area (S_{BET}) was determined using the standard Brunauer–Emmett–Teller method [31] on the basis on the adsorption data. The elemental composition of the surface particles was examined with Energy Dispersive X-ray Spectrometer (Genesis, EDX) using a voltage of 20 kV.

2.3. Catalytic testing

The catalytic testing of the ferrite catalysts in the flameless combustion of some selected VOCs (acetone, propane and benzene) was carried out at atmospheric pressure in a flow-type set-up (flow rate of 100 cm^3/min and VOC concentration in air of 1–2‰) previously described by us in [32,33]. The catalyst powder (0.3–0.5 g) was sandwiched between two layers of quartz wool in a quartz tubular micro-reactor (Ø = 7 mm) placed in an electrical furnace. The increase of the temperature was made in steps of 50 °C, from 50 °C to 550 °C. At every predetermined temperature, as a result of catalytic combustion, the gas concentration at the exit of reactor will be smaller than the inlet gas concentration. The catalytic activity of the ferrite catalysts under study was evaluated in terms of the conversion degree of gases over catalysts calculated as:

$$\text{Conv} = \frac{c_{in} - c_{out}}{c_{in}} \times 100\%,$$

where c_{in} and c_{out} are the inlet and outlet gas concentration, respectively, measured by a photo-ionization detector (PID-TECH) for VOCs. Data were collected when the flameless catalytic combustion had reached a steady state, after about 20 min at each temperature. These experiments were repeated decreasing the temperature and similar results were obtained suggesting the stability of the ferrites.

3. Results and discussion

3.1. Structural characterization

The XRD patterns of the Ni–Co ferrites with different molar substitutions of Sc^{3+} are shown in Fig. 1. Well-defined sharp peaks of the spinel phase clearly seen in the diffraction patterns indicate a good crystalline quality of the ferrite powders. The XRD patterns were compared and indexed using PDF no (44-1485) and (22-1086) for Ni and Co ferrites. The (2 2 0), (3 1 1), (2 2 2), (4 0 0), (4 2 2), (5 1 1) and (4 4 0) peaks reveal that all samples have the cubic spinel phase with Fd3m space group, without any foreign phase. A notable feature in these patterns is that the broadening of the peaks increases continuously with increasing scandium substitution in relation to the ferrite without scandium, indicating that the scandium addition reduces the crystallite size of the Co–Ni ferrite. The lattice parameters, average crystallite size and X-ray density derived from XRD data are given in Table 1. One can observe an increase in the lattice parameter with Sc content in Ni–Co ferrites from 8.36 Å for $x = 0$–8.41 Å for $x = 0.2$ and this may be explained by the higher ionic radius of Sc^{3+} compared to Fe^{3+} [30]. This result proves that the Sc^{3+} ions entered into the spinel structure and did not form a secondary phase during the sintering. The lattice parameter of sample without Sc is in agreement with that reported by others for Ni–Co ferrites [34,35]. Also, one can observe that sol–gel self-combustion preparing method allowed the synthesis of the ferrites with nanometer

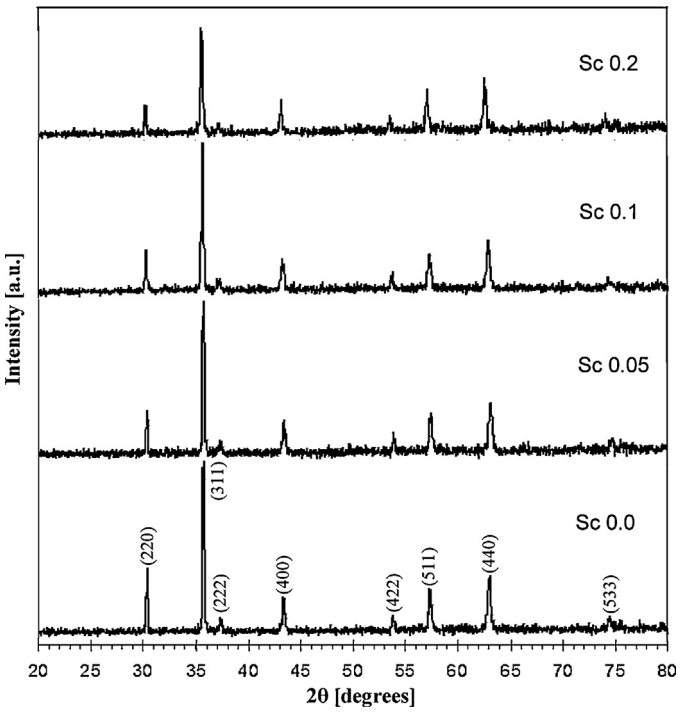

Fig. 1. XRD patterns of $Ni_{0.5}Co_{0.5}Sc_xFe_{2-x}O_4$ ferrite powders after heat treatment at 900 °C for 4 h.

size crystallites. Using the Scherrer equation, the average crystallite sizes were determined to be between 34.8 nm and 41.7 nm, proving the fine nature of the powders. The average crystallite size slowly decreased with the Sc incorporation and a probable explanation may be a structural disorder induced by the large Sc ions which can lead to a delay in the crystallite growth. This can also explain why the partial replacement of iron by scandium results in a progressive increase of the specific surface area, S_{BET}, with the Sc content, as can be seen in Table 1. The largest value (32.3 m^2/g) of S_{BET} was obtained for $Ni_{0.5}Co_{0.5}Sc_{0.2}Fe_{1.8}O_4$ ferrite composition. Similar values of S_{BET} for Ni–Co ferrites were reported in literature [34].

The X-ray density d_X, (calculated from the molecular weight and the volume of the unit cell, using the relation $d_X = 8M/Na^3$, where M is molecular weight, N is Avogadro's number and a is lattice parameter) was slightly modified, from 5.43 g/cm^3 to 5.33 g/cm^3, by Sc insertion (Table 1).

The surface elemental composition of the monophasic ferrospinel samples was checked by EDX analysis. The EDX patterns evidenced the presence of Fe, Co, Ni, Sc and O elements and no other impurity element. The elemental composition is given in Table 2. Each composition represents the mean value of six determinations in different points of each sample. The results given in Table 2 reveal the followings: (i) There is a difference between samples regarding the Ni and Co surface content. (ii) The Fe/(Ni + Co + Fe + Sc), Ni/(Ni + Co + Fe + Sc), Co/(Ni + Co + Fe + Sc) and Sc/(Ni + Co + Fe + Sc) ratios are found to be different, to some extent, to those determined on the basis of nominal composition (given in parenthesis in Table 2). (iii) The atomic ratio of Co/(Ni + Co + Fe + Sc) reveals a surface enrichment of Co at the expense of Fe (see Fe/(Ni + Co + Fe + Sc) ratio) and this may suggest a possible migration of Co ions from bulk of solid toward their surface during the heat treatment. These findings indicate a heterogeneous nature of investigated ferrites, i.e. the chemical composition of the bulk is different from that of their surface (surface particles).

Table 1
Lattice parameter (a), average crystallite size (D_{XRD}), X-ray density (d_X) and specific surface area (S_{BET}) of $Ni_{0.5}Co_{0.5}Sc_xFe_{2-x}O_4$.

x	a (nm)	D_{XRD} (nm)	d_X (g/cm^3)	S_{BET} (m^2/g)
0.00	0.8365	41.7	5.43	26.5
0.05	0.8375	38.8	5.38	28.7
0.10	0.8399	35.2	5.35	31.7
0.20	0.8413	34.8	5.33	32.3

The morphology of the ferrites without and with scandium substitution (for $x = 0$, 0.1 and 0.2) can be observed in the SEM images given in Fig. 2. These micrographs reveal that, in all the studied systems, the nanometric particles (<100 nm) cluster into soft agglomerates. Costa et al. [9] also reported a morphology consisting of soft agglomerates of nanoparticles smaller than 100 nm in Ni–Cu–Zn ferrites. There are no large agglomerates in Sc doping samples and the particle sizes are smaller. Although the nanoparticles are agglomerated, some individual particles with size below 50 nm can be observed (Fig. 2d).

3.2. Catalyst activity

The catalyst activity of the prepared ferrospinels was tested in catalytic combustion of propane, acetone and benzene within the 50–550 °C temperature range at total GHSV of 5100 h^{-1}. The results are given in Fig. 3, where the measured values of gas conversion are plotted as a function of the reaction temperature. Each datum is the average of three steady state measurements.

Typical S-shaped curves were obtained, describing the variation of the conversion degree with increase of the reaction temperature of the catalysts. These curves indicate that the catalytic activity of the materials is strongly influenced by the reaction temperature. No catalytic activity was observed at temperatures below 100 °C. Increasing the reaction temperature promotes gas conversion over the four ferrite catalysts. In Fig. 3 it is obvious a temperature shift of the S-curves by Sc incorporation in Ni–Co ferrite. This shift to lower temperatures is more pronounced in the range of medium conversions and for larger Sc content ($x = 0.2$). Compared to $Ni_{0.5}Co_{0.5}Fe_2O_4$, the Sc doped Ni–Co ferrite catalysts are more active in the gas oxidation and their catalytic activity increased substantially with an increase in Sc substitution. The effect of Sc content is more evident in propane combustion. Fig. 4 plots the conversion degree of the three gases measured at 300 °C as a function of Sc content in ferrites. One can remark that the gas conversion on the Sc doped Ni–Co ferrites increased with the increase in Sc amount and for $x = 0.2$ the highest conversions were achieved for propane and acetone. Over $Ni_{0.5}Co_{0.5}Sc_{0.2}Fe_{1.8}O_4$ ferrite catalyst the propane conversion is 80%, whereas over pure Ni–Co ferrite the propane conversion is 50% only at 300 °C. The increase by 60% of the propane conversion by Sc doping of Ni–Co ferrite may be ascribed to the structural defects induced by Sc substitution for iron (Table 1). For benzene, the activity of Ni–Co ferrites is quite poor at 300 °C. However the Sc substitution for Fe determined a slight increase of the benzene conversion.

To estimate the catalytic activity of a catalyst, the temperature required for 50% gas conversion, T_{50}, is usually chosen as main indicator of catalytic activity of a given catalyst. At T_{50}, the catalytic activity is sufficiently high and the interactions between catalyst surface and reactants are intense. The lower T_{50} is, the higher is the catalytic activity of a catalyst. From Fig. 5 it is clear the effect of Sc on the T_{50} and implicitly, on the catalytic activity of the catalysts. T_{50} decreased with the increase of Sc content. In addition, one can remark that T_{50} temperature for propane or acetone is much lower compared to that for benzene. Taking the T_{50} into account, the $Ni_{0.5}Co_{0.5}Sc_{0.2}Fe_{1.8}O_4$ catalyst appears to be the most active catalyst on which the combustion of acetone can reach 90% conversion at 350 °C. The catalytic performance of this catalyst is comparable

Table 2
EDX analysis of $Ni_{0.5}Co_{0.5}Sc_xFe_{2-x}O_4$ ferrites.

x	O (at%)	Ni (at%)	Co (at%)	Sc (at%)	Fe (at%)	Fe/M_t	Ni/M_t	Co/M_t	Sc/M_t
0.00	57.16	7.80	8.06	0	26.98	0.630 (0.667)	0.182 (0.166)	0.188 (0.166)	0
0.05	51.54	8.62	10.40	0.69	28.74	0.593 (0.650)	0.178 (0.166)	0.213 (0.166)	0.016 (0.017)
0.10	52.25	7.29	9.75	1.21	29.49	0.617 (0.633)	0.153 (0.166)	0.204 (0.166)	0.025 (0.033)
0.20	49.39	8.09	9.82	3.34	29.36	0.580 (0.600)	0.160 (0.166)	0.194 (0.166)	0.066 (0.067)

M_t is total amount of metallic composition (Ni + Co + Fe + Sc) on the surface. In parenthesis are given theoretical values.

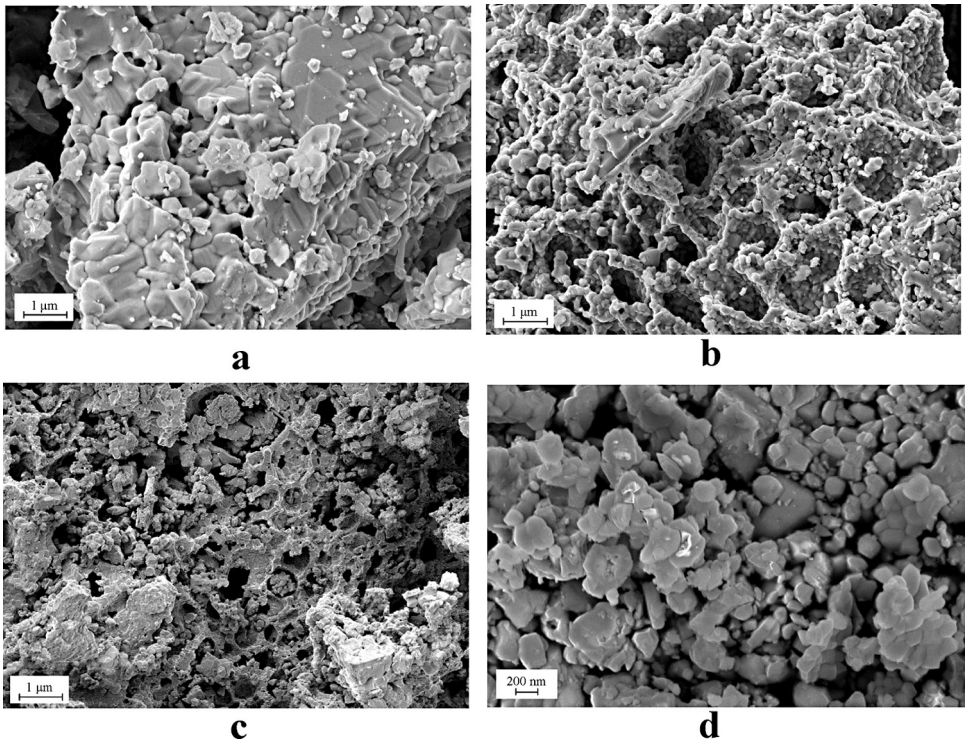

Fig. 2. SEM micrographs for $Ni_{0.5}Co_{0.5}Sc_xFe_{2-x}O_4$ nanopowders: (a) $x = 0.0$; (b) $x = 0.1$; (c and d) $x = 0.2$ (notice a difference in magnification).

to that of Pt/Al_2O_3 catalyst which could achieve the 95% conversion of acetone at 300 °C [36].

The long term activity test was carried out in this work for $Ni_{0.5}Co_{0.5}Sc_{0.2}Fe_{1.8}O_4$ catalyst using propane gas only. The reaction temperature was set at 350 °C. By a continuous operation of the reactor for about 40 h while periodically monitoring the conversion, very small variations were obtained. As shown in Fig. 6, the conversion of propane was maintained approximately constant (of about 90%) during the following 40 h, without any deactivation of the catalyst, confirming that the $Ni_{0.5}Co_{0.5}Sc_{0.2}Fe_{1.8}O_4$ ferrite is an active and stable catalyst.

An interesting observation is that the four ferrites are more active catalysts for acetone and propane combustion on which conversions higher than 80% were obtained. Thus, at 400 °C (Fig. 3 and Table 3) the acetone or propane conversion is of about 90%, whereas the benzene conversion is below 50%, either over ferrite catalysts with or without Sc. The reasons for such a selective catalytic activity of Ni–Co ferrites are not yet clear.

In Table 3 are included the values of the kinetic parameters (apparent activation energy, E_{app}, and reaction rate) for gas oxidation over the four ferrite catalysts.

The apparent activation energies (E_{app}) of the ferrite catalysts for the catalytic combustion reaction of propane, acetone, and benzene were estimated from linear Arrhenius plots for low conversion regions (below 15%). As shown in Table 3, substituted ferrites present lower activation energy in comparison with that of unsubstituted ferrite. The smallest value of E_{app} for $x = 0.2$ offers an explanation for the best catalytic activity of $Ni_{0.5}Co_{0.5}Sc_{0.2}Fe_{1.8}O_4$ ferrite. The values of activation energy obtained by us are comparable to those presented by others authors for other spinel ferrites and VOCs [12,13]. The E_{app} values fall within the commonly range of 50–95 KJ/mol and this suggests that the mechanism of the catalytic reaction did not change for $Ni_{0.5}Co_{0.5}Sc_xFe_{2-x}O_4$ catalysts with different Fe content. The difference in the catalytic activity may result from a variation in the number of active sites or the amount of

Table 3
Gas conversion at 400 °C, apparent activation energies (E_{app}) and reaction rate at 200 °C for catalytic combustion of propane, acetone and benzene over $Ni_{0.5}Co_{0.5}Sc_xFe_{2-x}O_4$ catalysts.

Gas	x	Gas conversiom (%)	Activation energy (KJ/mol)	Reaction rate ($\mu mol\ s^{-1}\ m^{-2}$)
Propane	0.00	86.3	81.7	4.57×10^{-2}
	0.05	85.4	76.6	4.63×10^{-2}
	0.10	87.5	64.7	4.66×10^{-2}
	0.20	90.5	50.0	5.53×10^{-2}
Acetone	0.00	87.3	80.0	1.35×10^{-2}
	0.05	88.7	72.1	2.18×10^{-2}
	0.10	90/0	64.4	–
	0.20	92.3	53.1	3.87×10^{-2}
Benzene	0.00	37.2	95.5	0.84×10^{-2}
	0.05	40.0	80.2	1.36×10^{-2}
	0.10	44.0	74.4	1.76×10^{-2}
	0.20	51.0	69.1	2.42×10^{-2}

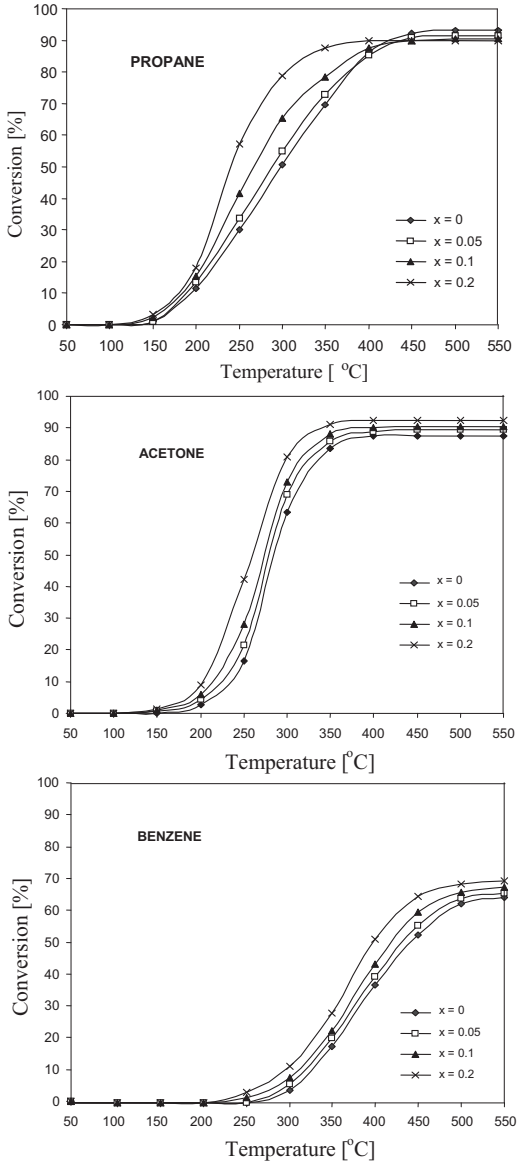

Fig. 3. Temperature dependence of propane, acetone and benzene conversion over $Ni_{0.5}Co_{0.5}Sc_xFe_{2-x}O_4$ ferrite catalysts.

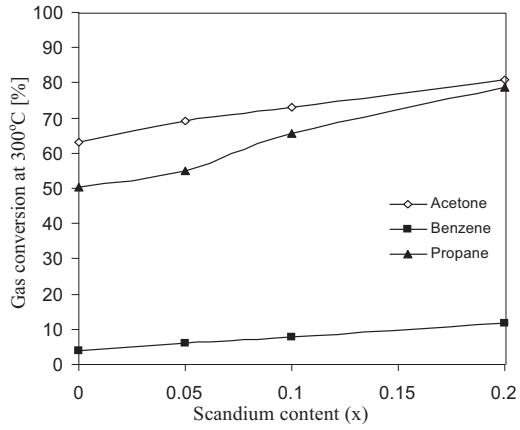

Fig. 4. Effect of Sc content (x) in $Ni_{0.5}Co_{0.5}Sc_xFe_{2-x}O_4$ ferrite catalysts on the conversion at 300 °C for propane, acetone and benzene combustion.

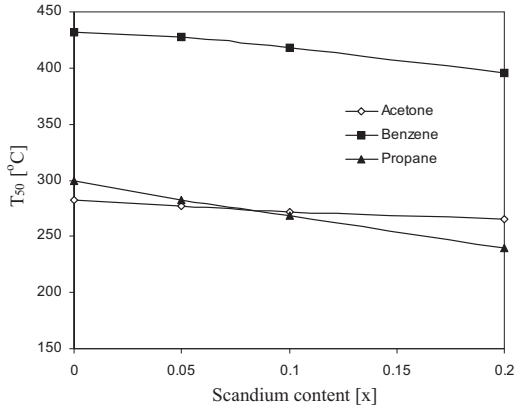

Fig. 5. Effect of Sc content (x) in $Ni_{0.5}Co_{0.5}Sc_xFe_{2-x}O_4$ ferrite catalysts on T_{50} temperature required for 50% conversion of propane, acetone and benzene.

surface active oxygen species involved in the oxidation reaction of gases over oxide compounds. The reaction rate normalized to specific surface area can characterize the specific catalytic activity of the catalysts. A catalyst is more active with higher reaction rates. The reaction rates per square meter of catalyst are given to better ascertain the potentiality of the catalysts compared in this work. Table 3 shows that the reaction rate substantially changes from 0.84×10^{-2} μmol s^{-1} m^{-2} to 5.50×10^{-2} μmol s^{-1} m^{-2} in terms of catalyst composition or gas type. The effect of Sc doping on the reaction rate and implicitly, on the catalytic activity of the Ni–Co ferrite catalyst, is apparent. The highest value of the reaction rate (5.50×10^{-2} μmol s^{-1} m^{-2}) was obtained for propane combustion over the $Ni_{0.5}Co_{0.5}Sc_{0.2}Fe_{1.8}O_4$ catalyst composition, which proved the best catalytic activity in the propane combustion (90% conversion degree at 400 °C). The lowest value of the reaction rate (0.84×10^{-2} μmol s^{-1} m^{-2}) was obtained for benzene combustion over the Sc-free ($x = 0$) Ni–Co ferrite catalyst. This Sc-free catalyst proved the worst catalytic activity in the benzene conversion (65% conversion degree at 550 °C) as can be seen in Fig. 3.

The data obtained by us allowed to conclude that the partial Sc substitution for iron in $Ni_{0.5}Co_{0.5}Fe_2O_4$ has a promotion effect on the catalytic activity of these oxide compounds within the temperature range explored.

In the present study, the better catalyst performance of Sc containing Ni–Co ferrites compared to pure Ni–Co ferrite may be attributed to smaller crystallite size, larger surface area and the presence of Sc cations in the cubic spinel structure of ferrite. The increase of the specific surface area by Sc incorporation implies more interactions between catalyst surface and test gases, promoting the gas oxidation at lower temperatures. The partial replacement of iron by scandium on octahedral sites of the spinel

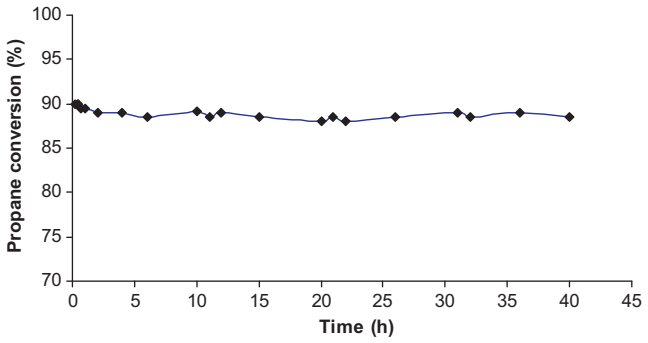

Fig. 6. Time evolution of propane conversion over $Ni_{0.5}Co_{0.5}Sc_{0.2}Fe_{1.8}O_4$ catalyst (2‰ propane in air, 0.5 g catalyst) at 350 °C.

structure can generate, due to the large difference between their ionic radii, during the heat treatment at 900 °C, structural defects in the form of vacancies which play a favorable role in the oxidation process of gases. More oxygen vacancies will involve a larger density of active oxygen species adsorbed on ferrite surface. Although the mechanism of complete gas oxidation over metal oxide compounds is not known accurately, the interaction of surface active oxygen species with reactants ("suprafacial mechanism") is widely accepted to explain VOCs full oxidation over oxide catalysts for $T < 400$ °C [37,38]. The larger the number of oxygen ions adsorbed, the faster would be the oxidation of gases. In addition, the oxygen vacancies facilitate the mobility of the lattice oxygen from bulk to surface (via oxygen vacancy mechanism [39]) and the ferrite catalyst will be more active for oxidation reactions of gases [40].

The results underline the need of further investigations to clarify the role of Sc^{3+} ion on the catalytic performance of Ni–Co ferrites in the catalytic combustion of VOCs.

4. Conclusions

In this work, the combined sol–gel and self-combustion method has been employed to prepare $Ni_{0.5}Co_{0.5}Sc_xFe_{2-x}O_4$ ($x = 0$, 0.05, 0.1 and 0.2) ferrospinels for catalytic applications. It is a fast and inexpensive method and the obtained products were monophasic and presented nanosized crystallinity (35–42 nm).

All samples have been tested in the catalytic flameless combustion of acetone, propane and benzene to estimate the effect of Sc ions on the catalytic activity of $Ni_{0.5}Co_{0.5}Fe_2O_4$ ferrite.

The results revealed that the partial substitution of Fe^{3+} by Sc^{3+} ions on the octahedral sites in spinel structure of $Ni_{0.5}Co_{0.5}Fe_2O_4$ ferrite has a favorable effect on the catalytic activity of this ferrite. The $Ni_{0.5}Co_{0.5}Sc_{0.2}Fe_{1.8}O_4$ ferrite composition was found to be the most active catalyst and can be a good candidate for catalytic combustion of propane or acetone at moderate temperatures. Over this catalyst the conversion degree of acetone or propane can exceed 90% at 400 °C. The improved catalytic activity of the Sc doped Ni–Co ferrites compared to pure Ni–Co ferrite may be ascribed to smaller crystallite sizes (35–39 nm), larger specific surface areas (29–32 m^2/g) and the presence of Sc cations in the octahedral sites of spinel structure of the ferrite.

Acknowledgment

This work was supported by a grant of the Romanian National Authority for Scientific Research, CNST–UEFISCDI, project number PN-II-ID-PCE-2011-3-0453.

Appendix A. Supplementary data

Supplementary data associated with this article can be found, in the online version, at http://dx.doi.org/10.1016/j.apcatb.2014.03.052.

References

[1] Z. Fan, P. Lioy, K. Veschler, N. Fiedler, H. Kipen, J. Zhang, Environ. Sci. Technol. 37 (2003) 1811–1921.
[2] W.B. Li, W.B. Chu, M. Zhuang, J. Hua, Catal. Today 93–95 (2004) 205–209.
[3] W.B. Li, J.X. Wang, H. Gong, Catal. Today 148 (2009) 81–87.
[4] K. Everaert, J. Baeyens, J. Hazard. Mater. B 109 (2004) 113–139.
[5] E.C. Njagi, H.C. Genuino, C.K. King'ondu, S. Dharmarathna, S.L. Suib, Appl. Catal. A: Gen. 421–422 (2012) 154–160.
[6] M.S. Sadjadi, M. Mozaffari, M. Enhessari, K. Zare, Superlat. Microst. 47 (2010) 685–694.
[7] M. Epifani, E. Melissano, G. Pace, M. Schiopa, J. Eur. Ceram. Soc. 27 (2007) 115–123.
[8] A.V. Murugan, V. Samuel, S.C. Navale, V. Ravi, Mater. Lett. 60 (2006) 1791–1792.
[9] A.C.F.M. Costa, R.T. Lula, R.H.G.A. Kiminami, L.F.V. Gama, A.A. de Jesus, H.M.C. Andrade, J. Mater. Sci. 41 (2006) 4871–4875.
[10] N. Rezlescu, E. Rezlescu, P.D. Popa, E. Popovici, C. Dorogtei, M. Ignat, Mater. Chem. Phys. 137 (2013) 922–927.
[11] M.R. Morales, B.P. Barbero, L.E. Cadus, Fuel 87 (2008) 1177–1186.
[12] A. Urda, A. Herraïz, A. Rédey, I.C. Marcu, Catal. Commun. 10 (2009) 1651–1655.
[13] M. Florea, M. Alifanti, V.I. Parvulescu, D. Mihaila-Tarabasanu, L. Diamandescu, M. Feder, C. Negrila, L. Frunza, Catal.Today 14 (2009) 361–366.
[14] A.S. Albuquerque, M.V.C. Tolentino, J.C. Alrdisson, F.C.C. Moura, Renato de Mendonça, W.A.A. Macedom, Ceram. Int. 38 (2012) 2225–2231.
[15] C.G. Ramankutty, S. Sugunan, Appl. Catal. A: Gen. 218 (2011) 39–51.
[16] A. Goldman, Modern Ferrite Technology, second ed., Pittsburg, Spriger, 2006.
[17] J.P. Jacobs, A. Maltha, J. Drimal, V. Ponec, H.H. Brongersma, J. Catal. 47 (1994) 294–300.
[18] N. Chu, X. Wang, Y. Liu, H. Jin, Q. Wu, L. Li, Z. Wang, H. Ge, J. Alloys Compd. 470 (2009) 438–442.
[19] A.B. Gadkari, T.J. Shinde, P.N. Vasambekar, Mater. Chem. Phys. 114 (2009) 505–510.
[20] C.V. Gopal Reddy, S.V. Manorama, V.J. Rao, Sens. Actuators B: Chem. 55 (1999) 90–95.
[21] P.A. Jadhav, R.S. Devan, Y.D. Kolekar, B.K. Chougule, J. Phys. Chem. Solids 70 (2009) 396–400.
[22] S. Prasad, N.S. Gajbhiye, J. Alloys Compd. 265 (1998) 87–92.
[23] S. Komarneni, E. Fregeau, E. Breval, R. Roy, J. Am. Ceram. Soc. Commun. 71 (1988) C26–C28.
[24] X. Li, G. Wang, J. Magn. Magn. Mater. 321 (2009) 1276–1282.
[25] R.V. Mangalaraja, S. Thomas Lee, S. Ananthakumar, P. Manohar, C.P. Camurri, Mater. Sci. Eng. A: Struct. 476 (2008) 234–239.
[26] Z. Lei, Y. Sun, M.-F. Han, Q.-B. Wang, Acta Phys. Chim. Sin. 28 (2012) 2129–2134.
[27] S.A. Hosseini, A. Niaei, D. Salari, F. Aghzadeh, Chin. J. Chem. 28 (2010) 143–148.
[28] N.I. Pakhomova, G.I. Granik, L.A. Presnova, R.A. Shilova, Sov. Phys. J. 17 (1974) 672–676.
[29] P.D. Popa, N., Rezlescu, Gh. Iacob, A new procedure for preparing ferrite powders, Romanian Patent No. 121300, OSIM, Bucharest, 2008.
[30] J.E. Huheey, E.A. Keiter, R.J. Keiter, Chemistry Principles of Structure and Reactivity, Harper Collins, College Publishers, New York, 1993.
[31] S. Lowell, J.E. Shields, M.A. Thomas, M. Thommes, Characterization of Porous Solids and Powders: Surface Area, Pore Size and Density, Kluwer Academic Publishers, Dordrecht/Boston/London, 2004.
[32] N. Rezlescu, E. Rezlescu, P.D. Popa, C. Doroftei, M. Ignat, J. Mater. Sci. 48 (2013) 4297–4304.
[33] N. Rezlescu, E. Rezlescu, L. Sachelarie, P.D. Popa, C. Doroftei, Catal. Commun. 46 (2014) 51–56.
[34] R. Hosseini Akbarnejad, V. Daadmehr, A.T. Rezakhani, F. Shahbaz Tehrani, F. Aghakhani, S. Gholipour, J. Supercond. Nov. Magn. 26 (2013) 429–435.
[35] L.A. Alekseyuk, Sov. Powder Metall. 8 (1959) 463–465.
[36] N. Burgos, M. Paulis, M.M. Antxustegi, M. Montes, Appl. Catal. B: Environ. 38 (2002) 251–258.
[37] D.V. Ivanov, L.G. Pinaeva, E.M. Sadovskaya, L.A. Isupova, Kinet. Catal. 52 (2011) 401–408.
[38] D. Hirabayashi, T. Yosikawa, Y. Kawamoto, K. Mockizuki, K. Suzuki, Adv. Sci. Technol. 45 (2006) 2169–2175.
[39] A.A. Taskin, A.N. Lavrov, Y. Ando, Prog. Solid State Chem. 35 (2007) 481–490.
[40] H. Arai, H. Fukuzawa, Catal. Today 26 (1995) 217–221.